Appl. Math. Mech. -Engl. Ed., **37**(11), 1467–1478 (2016)
DOI 10.1007/s10483-016-2106-8

Applied Mathematics and Mechanics (English Edition)

Numerical simulation based on two-directional freeze and thaw algorithm for thermal diffusion model*

Junqiang GAO[1,2], Zhenghui XIE[1,†], Aiwen WANG[3], Zhendong LUO[2]

1. State Key Laboratory of Numerical Modeling for Atmospheric Sciences and Geophysical Fluid Dynamics, Institute of Atmospheric Physics, Chinese Academy of Sciences, Beijing 100029, China;
2. School of Mathematics and Physics, North China Electric Power University, Beijing 102206, China;
3. School of Applied Science, Beijing Information and Science Technology University, Beijing 100192, China

Abstract Freeze-thaw processes significantly modulate hydraulic and thermal characteristics of soil. The changes in the frost and thaw fronts (FTFs) affect the water and energy cycles between the land surface and the atmosphere. Thus, the frozen soil comprising permafrost and seasonally frozen soil has important effects on the land surface hydrology in cold regions. In this study, a two-directional freeze and thaw algorithm is incorporated into a thermal diffusion equation for simulating FTFs. A local adaptive variable-grid method is used to discretize the model. Sensitivity tests demonstrate that the method is stable and FTFs can be tracked continuously. The FTFs and soil temperature at the Qinghai-Tibet Plateau D66 site are simulated hourly from September 1, 1997 to September 22, 1998. The results show that the incorporated model performs much better in the soil temperature simulation than the original thermal diffusion equation, showing potential applications of the method in land-surface process modeling.

Key words freeze and thaw algorithm, frost and thaw front (FTF), sensitivity test, thermal diffusion equation

Chinese Library Classification O242.1
2010 Mathematics Subject Classification 65M06

1 Introduction

Frozen soil (which comprises permafrost and seasonally frozen soil) plays an important role in the land surface hydrology of cold regions. Freeze-thaw processes significantly modulate the hydraulic and thermal characteristics of soil. Frost and thaw fronts (FTFs) separate a soil column into frozen and unfrozen segments, and the changes in the FTFs will affect the water and energy cycles between the land surface and the atmosphere.

* Received Jan. 26, 2016 / Revised Jun. 20, 2016
Project supported by the National Natural Science Foundation of China (Nos. 41575096 and 91125016) and the Strategic Priority Research Program of the Chinese Academy of Sciences (No. XDA05110102)
† Corresponding author, E-mail: zxie@lasg.iap.ac.cn

Permafrost (the ground that remains at or below 0 °C for at least two consecutive years) and seasonally frozen ground areas account for more than 30% of the Earth's total land area[1]. In particular, the area with frozen soil is equivalent to 75% of the land surface in China, and the permafrost is distributed mainly on the Qinghai-Tibet Plateau and in the northeast of China. The maximum frost depth is an important parameter when roadbeds in seasonally frozen areas are designed[2–5]. Frozen soils have a limited capacity for infiltration which leads to high levels of runoff during the spring snowmelt[6–7]. Moreover, the thaw depth of the soil is important for cultivation and seeding during early spring[8]. Changes in the depths of the FTFs can affect ecosystems via carbon cycling. Thus, the organic matter decomposition rate in the unfrozen soil is ten times larger than that in frozen soils in the black spruce forest[9]. The increased respiration rate of soil can be explained by the increases in the thaw depth during mid-summer. The FTF depth is sensitive to the climate change, and it is an important indicator of the climate change[10].

Interpolating the soil temperature (observed or simulated) and obtaining the position of the freezing and thawing point T_{f} isotherm are a typical method for estimating the depth of FTFs. However, multiple FTFs cannot be simulated in the same soil layer by use of this method. In addition, this method will produce numerical oscillations when the soil temperature is close to the freezing temperature T_{f} during the autumn freezing and spring snowmelt periods.

The Stefan equation[11] can be used to calculate the FTFs in a one-directional soil column, where this method assumes that all of the heat reaching the FTFs can be used for freezing the soil water or for melting the soil ice. Little site-specific information is available. Therefore, the Stefan solution can be used frequently by permafrost scientists to predict the frost depth and to simulate the heat transfer during water phase transitions in the frozen soil[12–14]. Woo et al.[15] used the surface and deep soil temperature as forcing variables in the Stefan equation, and proposed a two-directional freeze and thaw algorithm.

Significant studies of soil freezing and thawing processes have been performed since the 1970s when Harlan[16] constructed the first hydrothermal coupled-migration model. Based on field observations and laboratory experiments, soil water and heat coupling models as well as their corresponding numerical simulation algorithms have been developed for different needs[17–21]. These studies have advanced the study of soil hydrothermal processes. However, they have not considered changes in the depth of FTFs and their influence on the model.

In this study, we use a two-directional freeze and thaw algorithm to simulate changes in the FTF depth, where this method is incorporated into the thermal diffusion equation. In the version 4.5 of the Community Land Model (CLM), the thermal diffusion equation is used to simulate the temperature for a 15-layer soil column. A local adaptive variable-grid method is used to discretize the model. The results of sensitivity tests demonstrate that this method is stable and the FTFs can be tracked continuously. The present simulation of the Qinghai-Tibet Plateau D66 site shows that the incorporated model performs much better in the soil temperature simulation than the original thermal diffusion equation. The soil temperature profile within a soil layer can be estimated according to the position of the freezing front, thereby demonstrating the potential application of this method to land-surface process modeling.

2 Thermal diffusion model including changes of FTFs

2.1 Thermal diffusion equation

We consider the simulation of a one-dimensional vertical soil column. Let $(0, L)$ be the one-dimensional vertical soil column, $z = 0$ be the top of the soil column, and $z = L$ be the bottom of the soil column. We assume that the position of the freezing and thawing point T_{f} isotherm is defined as the position of the soil FTF.

Based on the energy conservation, the thermal diffusion equation can be written as follows:

$$C\frac{\partial T}{\partial t} = -\frac{\partial F}{\partial z}, \tag{1}$$

$$F = -\lambda\frac{\partial T}{\partial z}, \tag{2}$$

where t (s) is the time, z (m) is the space coordinate (positive downward), $C\,(\mathrm{J{\cdot}m^{-3}{\cdot}K^{-1}})$ is the soil heat capacity, $\lambda\,(\mathrm{W\cdot m^{-1}\cdot K^{-1}})$ is the soil thermal conductivity, T (K) represents the soil temperature, and F $(\mathrm{W\cdot m^{-2}})$ is the heat flux.

The soil heat capacity $C\,(\mathrm{J\cdot m^{-3}\cdot K^{-1}})$ is calculated as follows:

$$C = C_{\mathrm{g}}(1-\theta_{\mathrm{s}}) + C_{\mathrm{w}}\theta_{\mathrm{w}} + C_{\mathrm{i}}\theta_{\mathrm{i}}, \tag{3}$$

where θ_{s} is the soil porosity, and $C_{\mathrm{g}}, C_{\mathrm{w}}$, and C_{i} represent the volumetric heat capacities of soil solid, water, and ice, respectively.

In Eq. (3), C_{g} can be calculated as

$$C_{\mathrm{g}} = \Big(\frac{2.128P_{\mathrm{s}} + 2.385P_{\mathrm{c}}}{P_{\mathrm{s}} + P_{\mathrm{c}}} + P_{\mathrm{c}}\Big)\times 10^{6}, \tag{4}$$

where P_{s} and P_{c} are the percentages of the sand and the clay in the soil, respectively.

The soil thermal conductivity λ can be calculated as

$$\lambda = Ke(\lambda_{\mathrm{sat}} - \lambda_{\mathrm{dry}}) + \lambda_{\mathrm{dry}}, \tag{5}$$

where Ke is the Kersten number, which can be calculated as follows:

$$\begin{cases} 0.7\lg S_{\mathrm{r}} + 1.0 \geqslant 0, & T \geqslant T_{\mathrm{f}}, \\ S_{\mathrm{r}}, & T < T_{\mathrm{f}}, \end{cases} \tag{6}$$

where

$$S_{\mathrm{r}} = \frac{\theta_{\mathrm{i}} + \theta_{\mathrm{w}}}{\theta_{\mathrm{s}}} \leqslant 1. \tag{7}$$

The saturated soil thermal conductivity λ_{sat} and the dry soil thermal conductivity λ_{dry} can be calculated as

$$\lambda_{\mathrm{sat}} = \lambda_{\mathrm{s}}^{1-\theta_{\mathrm{s}}}\lambda_{\mathrm{i}}^{\theta_{\mathrm{s}}-\theta_{\mathrm{w}}}\lambda_{\mathrm{l}}^{\theta}, \tag{8}$$

$$\lambda_{\mathrm{dry}} = \frac{0.135\rho_{\mathrm{d}} + 64.7}{2700 - 0.947\rho_{\mathrm{d}}}, \tag{9}$$

where $\lambda_{\mathrm{s}}, \lambda_{\mathrm{i}}$, and λ_{l} are the thermal conductivities of soil solid, ice, and water, respectively, ρ_{d} $(\mathrm{kg{\cdot}m^{-3}})$ is the bulk density, and Q is the volumetric fraction of the soil moisture content.

In Eq. (8), the thermal conductivity of soil solid λ_{s} can be calculated as

$$\lambda_{\mathrm{s}} = \frac{8.80P_{\mathrm{s}} + 2.93P_{\mathrm{c}}}{P_{\mathrm{s}} + P_{\mathrm{c}}}. \tag{10}$$

We use the following equation to calculate the supercooled water content when the soil temperature is less than T_{f}:

$$\theta_{\max} = \theta_{\mathrm{s}}\Big(\frac{L_{\mathrm{i}}(T_{\mathrm{f}} - T)}{g\psi_{\mathrm{s}}T_{\mathrm{f}}}\Big)^{-\frac{1}{b}}, \quad T < T_{\mathrm{f}}, \tag{11}$$

where $\theta_{\max}$ is the maximum liquid water when the soil temperature T is below the freezing temperature $T_{\rm f}$, g is the acceleration due to gravity, $\psi_{\rm s}$ is the saturated water potential, $L_{\rm i}$ is the latent heat of fusion, and b is the Hornberger exponent.

We assume that the heat flux is zero for the lower boundary conditions. The discretization of Eqs. (1) and (2) can be calculated as

$$\frac{c_i\Delta z_i}{\Delta t}(T_i^{n+1}-T_i^n)=\alpha(-F_{i-1}^n+F_i^n)+(1-\alpha)(-F_{i-1}^{n+1}+F_i^{n+1}), \tag{12}$$

$$F_i^n=-\lambda_i\frac{T_{i+1}^n-T_i^n}{z_{i+1}-z_i}, \tag{13}$$

where the parameter $\alpha=0.5$.

2.2 Calculation of FTFs

We use a two-directional freeze and thaw algorithm[15,22] to simulate the depth of the FTFs in the present study. First, we consider the case of downward freezing or melting.

The Stefan equation can be described in the following form:

$$z_l=\sqrt{\frac{2\lambda D}{L\theta}}, \tag{14}$$

$$D=(T-T_{\rm f})t, \tag{15}$$

where z_l ($l=$ f or t) (m) is the frost/thaw front depth, D (°C · s) is the freeze/thaw index, t is the freezing or thawing duration, T (°C) is the average temperature at the surface, and L (J · m^{-3}) is the volumetric latent heat of fusion.

Squaring the Stefan equation (14), we have

$$z_l^2=\frac{2\lambda D}{L\theta}, \tag{16}$$

and differentiating Eq. (15) for D, we have

$$2z_l\Delta z_l=\frac{2\lambda\Delta D}{L\theta}, \tag{17}$$

$$\Delta D=(L\theta\Delta z_l)\Big(\frac{z_l}{\lambda}\Big). \tag{18}$$

We assume that the thickness of the ith soil layer is Δz_i, the depth of the ith soil layer is z_i, the requirement of the freeze/thaw index for the frost/thaw front to pass from z_{i-1} to z_i is N_i, θ_i is the volumetric fraction of the ith layer soil moisture, and the thermal resistance of the ith layer soil is $R(i)=\Delta z_i/\lambda_i$.

If $z_{\rm f}=0$ when $t=0$, then for the first soil layer, $\Delta D=N_1$, $\Delta z_l=\Delta z_1$, and z_l changes from 0 to z_1. If we divide the first soil layer into N layers, then N_1 can be calculated as follows:

$$\begin{aligned}N_1&=\sum_{n=1}^{N}\Big(L\theta_1\frac{z_1}{N}\Big)\cdot\Big(\frac{nz_1}{N\lambda_1}\Big)\\&=(L\theta_1z_1)\Big(\frac{1}{2}\frac{N+1}{N}\frac{z_1}{\lambda_1}\Big)\\&=(L\theta_1z_1)\Big(\frac{1}{2}\frac{N+1}{N}R_1\Big).\end{aligned} \tag{19}$$

When $N\to\infty$,

$$N_1=(L\theta_1z_1)\Big(\frac{R_1}{2}\Big), \tag{20}$$

analogous to this rule,

$$\begin{cases} N_2 = (L\theta_2 z_2)\Big(R_1 + \dfrac{R_2}{2}\Big), \\ \quad \vdots \\ N_i = (L\theta_i z_i)\Big(\sum\limits_{n=1}^{i-1} R_n + \dfrac{R_i}{2}\Big). \end{cases} \tag{21}$$

When the freeze/thaw index $D \geqslant \sum\limits_{n=1}^{i-1} N_n$ and $D < \sum\limits_{n=1}^{i} N_n$,

$$D - \sum_{n=1}^{i-1} N_n = (L\theta_i \cdot z_{\mathrm{f}0})\Big(\sum_{n=1}^{i-1} R_n + \frac{z_{\mathrm{f}0}}{2\lambda_i}\Big), \tag{22}$$

where $z_{\mathrm{f}0}$ is the FTF depth in the ith soil layer.

By solving Eq. (21), we can obtain $z_{\mathrm{f}0}$ as

$$z_{\mathrm{f}0} = -\lambda_i \sum_{n=1}^{i-1} R_n + \Big(\lambda_i^2\Big(\sum_{n=1}^{i-1} R_n\Big)^2 + \Big(2\lambda_i\Big(D - \sum_{n=1}^{i-1} N_n\Big)/(L\theta_i)\Big)\Big)^{1/2}, \tag{23}$$

and the FTF depth is

$$z_l = z_{i-1} + z_{\mathrm{f}0}. \tag{24}$$

If $z_l > 0$, and $z_{i-1} < z_l \leqslant z_i$, when $t = 0$, then the freeze/thaw index can be used as follows to calculate the FTF depth:

$$D = \Big(\Big(z_l - z_{i-1} + \lambda_i \sum_{n=1}^{i-1} R_n\Big)^2 - \lambda_i^2\Big(\sum_{n=1}^{i-1} R_n\Big)^2\Big)\frac{L\theta_i}{2\lambda_i} + \sum_{n=1}^{i-1} N_n + (T - T_{\mathrm{f}})t. \tag{25}$$

The same approach is used for the upward calculations.

2.3 Numerical algorithm incorporating FTFs into thermal diffusion equation

If we assume that the soil temperature and the FTF depth are given at the time t_k, then the values of these variables at t_{k+1} can be calculated as follows[23–25]:

(i) Divide the soil column into n layers. The depth of the ith layer soil is z_i $(i = 1, 2, \cdots, n)$. The thickness of the ith layer soil is $\Delta z_i\,(i = 1, 2, \cdots, n)$. The soil heat capacity is C_i^k $(i = 1, 2, \cdots, n)$, and the soil thermal conductivity is $\lambda_i^k\,(i = 1, 2, \cdots, n)$. Assume that the temperature of the soil layers at the time t_k is $T_i^k\,(i = 1, 2, \cdots, n)$. The number of the frost depths is J_1, and the frost depth value is $z_{\mathrm{f},j_1}^k\,(j_1 = 1, 2, \cdots, J_1)$. The number of the thaw depths is J_2, and the thaw depth value is $z_{\mathrm{t},j_2}^k\,(j_2 = 1, 2, \cdots, J_2)$. If we assume that N FTFs satisfy the following conditions: $z_{\mathrm{f},j_1}^k - z_i > 0.02\Delta z_i$ and $z_{i+1} - z_{\mathrm{f},j_1}^k > 0.02\Delta z_i$, or $z_{\mathrm{t},j_2}^k - z_i > 0.02\Delta z_i$ and $z_{i+1} - z_{\mathrm{t},j_2}^k > 0.02\Delta z_i$, then we can obtain the initial values of the FTF depths by interpolating the initial soil temperature.

(ii) Add the number of nodes from n to $n + N$. Update $z_i, \Delta z_i$, and T_i^k to $z_m, \Delta z_m$, and $T_m^k\,(m = 1, 2, \cdots, n + N)$, respectively. If $z_m = z_{\mathrm{f},j_1}^k$ or $z_m = z_{\mathrm{t},j_2}^k$, then $T_m^k = 0\ ^\circ\mathrm{C}$. Interpolate the soil heat capacity C_i^k and the soil thermal conductivity λ_i^k to obtain C_m^k and λ_m^k.

(iii) As described in Subsection 2.1, calculate the soil temperature T_m^{k+1} at the time t_{k+1} for $n + N$ nodes with Eqs. (12) and (13). According to the corresponding relationship for $z_i\,(i = 1, 2, \cdots, n)$ and $z_m\,(m = 1, 2, \cdots, n + N)$, return the updated variable soil temperature which is from $T_m^{k+1}\,(m = 1, 2, \cdots, n + N)$ to $T_i^{k+1}\,(i = 1, 2, \cdots, n)$.

(iv) According to Subsection 2.2, calculate the frost front depth $z_{\mathrm{f},j_1}^{k+1}\,(j_1 = 1, 2, \cdots, J_1)$ and the thaw front depth $z_{\mathrm{t},j_2}^{k+1}\,(j_2 = 1, 2, \cdots, J_2)$ at the time t_{k+1} with Eqs. (22), (23), and (24). If $|z_{\mathrm{f},j_1}^{k+1} - z_{\mathrm{t},j_2}^{k+1}| \leqslant 0.01$, then $z_{\mathrm{f},j_1}^{k+1} = 0$, and $z_{\mathrm{t},j_2}^{k+1} = 0$.

(v) Return to repeat the step (i) to the step (iv).

3 Numerical experiments

3.1 Ideal test

To test and verify the correctness and numerical stability of the algorithm, the following sensitivity tests are performed. First, we compare the results of FTF simulations using two hypothetical soil profiles. Second, the FTF depths are simulated with different time steps and spatial resolutions. The details of the tests are described in the following.

3.1.1 Simulation of FTFs in multi-layered soil

The physical parameters of the two soil profiles are given in Table 1. Both of the profiles contain two soil layers, where the depths of the layers are 0.6 m and 1.5 m. Figure 1(a) is a homogeneous silt soil, and its properties remain constant with the depth. In Fig. 1(b), the upper layer is the silt soil, and the lower soil is the peat soil, which has a high water content and low thermal conductivity. In both cases, the surface temperature is the same, i.e., $T_{\rm surf} = -10$ °C. The initial frost depth values are both $z_{\rm f} = 0$, and the time step is $\Delta t = 3\,600$ s. We only consider the case of downward ground freezing.

Table 1 Physical parameters of soil profiles

	Soil type	Depth of soil layer/m	Bulk density /(kg·m^{-3})	Gravimetric water content	Unfrozen thermal conductivity/(W·m^{-1}·K^{-1})
Case 1	Silt	[0.0,0.6]	1 300	0.30	1.57
	Silt	[0.6,1.5]	1 300	0.30	1.57
Case 2	Silt	[0.0,0.6]	1 300	0.30	1.57
	Peat	[0.6,2.5]	680	0.70	0.57

Figure 1 shows the simulation results for the frost front depth in the two soil profiles. In both cases, the initial results are as expected. However, as the frost front moves through the interface between the two different layers, the frost front depth is deeper in Case 1. There is an abrupt change in the gradient in Case 2, which does not occur in Case 1. This is because the peat soil in Case 2 has a higher water content. Therefore, a lower temperature is required in the peat soil layer.

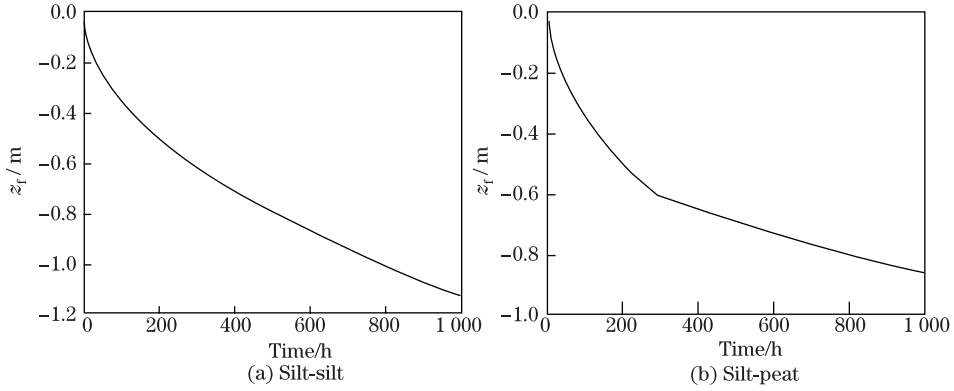

Fig. 1 Simulations of frost front depth in different soil profiles

In the common form of the Stefan equation, the thermal conductivity λ and the volumetric fraction of soil moisture θ are constants. Thus, this method is only suitable for the homogeneous soil. This test shows that the new algorithm reflects the physical properties of different soils. Based on these simulations, we conclude that our algorithm can be used for multi-layered soils.

3.1.2 Comparative test

We assume that the upper boundary condition is given by the following periodic temperature boundary condition:

$$T_{\text{surf}}(t) = 5\cos\Big(\frac{2\pi t}{1\ 000}\Big) + 2.$$

The initial values of the FTFs are $z_{\text{f}} = z_{\text{t}} = 0$. The soil hydraulic parameters are $\lambda_{\text{l}} = 0.57\ \text{W} \cdot \text{m}^{-1} \cdot \text{K}^{-1}$, $\lambda_{\text{i}} = 2.29\ \text{W} \cdot \text{m}^{-1} \cdot \text{K}^{-1}$, and $\lambda_{\text{s}} = 7.935\ 3\ \text{W} \cdot \text{m}^{-1} \cdot \text{K}^{-1}$[26]. The simulated volumetric water content is 0.3. The soil column, which is based on the hierarchical structure of the CLM[27], is discretized into 15 layers, where the depths of the nodes are

$$z_i = f_{\text{s}}(\exp(0.5(i - 0.5)) - 1),$$

and $f_{\text{s}} = 0.025$ is a scaling factor.

Under the experimental conditions described above, the following control tests are performed:

Test 1 The time steps are 0.5 h, 1 h, and 2 h, respectively. The spatial resolution is based on the hierarchical structure of the CLM. The FTFs are obtained as described in Subsection 2.2.

Test 2 The spatial resolution is based on the hierarchical structure of the CLM. The spatial resolution is set as a thickness of 1 cm for each soil layer. The time step is 1 h. We then simulate the FTF depths as described in Subsection 2.2.

Figure 2 shows the calculated results for different time steps and different spatial resolutions. Figures 2(a), 2(b), and 2(c) show the simulated results for the FTF depths at the three time steps. Using the results obtained at 1 h as a reference, the error in the calculated results at the other two time steps is shown in Fig. 2(d). The maximum error in the results at 0.5 h is 0.008 m, and the maximum error in the results at 2 h is 0.018 m. Figure 2(e) shows the simulated FTF depths at the high spatial resolution (the thickness of each soil layer is 1 cm). According to Fig. 2(f), the error in the results at different spatial resolutions is less than 0.006. These results demonstrate that the numerical algorithm is correct and stable.

3.2 Simulation test for Tibetan Plateau D66 site

The D66 site (35°31′N, 93°47′E) is located in the northern part of the Tibetan Plateau at an altitude of 4 560 m, where the precipitation is low, and the type of frozen soil is permafrost. The soil comprises 58% sand and 10% clay[19,28–29]. The observations obtained from the automatic weather station at D66 include atmospheric forcing fields at 1.5 m every 30 min. The soil temperatures in 10 layers (4 cm, 20 cm, 40 cm, 60 cm, 80 cm, 100 cm, 130 cm, 160 cm, 200 cm, and 250 cm) are obtained once each hour.

To verify the superior performance of the thermal diffusion model including the changes in the FTF depth proposed in this study, the following two models are tested:

Model 1 As described in Subsection 2.3, we incorporate the two-directional freeze and thaw algorithm into the thermal diffusion equation.

Model 2 As described in Subsection 2.1, we simulate the soil temperature using the original thermal diffusion equation.

In order to facilitate their comparison, the time step, the spatial resolution, the initial condition, and the boundary condition are all the same. The depth of the soil column is 2.5 m. The node depths are 4 cm, 20 cm, 40 cm, 60 cm, 80 cm, 100 cm, 130 cm, 160 cm, 200 cm, and 250 cm, and the time step is 1 h. The upper boundary condition and the initial soil temperature value are determined based on observations, and the lower boundary condition is assumed for the zero heat flux. The simulated time period ranges from September 1, 1997 to September 22, 1998.

Figure 3 shows the FTF depth changes during the simulation period according to Subsection 2.2, which we also compare with the observations obtained at the same time. The frost duration in the surface soil is up to about 5 months. As shown in Fig. 3, the freezing process occurs over about 3 months, and it reaches 250 cm in late December. The maximum observed depth is 250 cm, therefore, the maximum FTF depth is 250 cm in Fig. 3. The soil begins to thaw in early April, and the continuous thaw reaches down to 250 cm after almost 3 months. The correlation coefficients (CCs) for the frost front and thaw front in the simulations and observations are 0.79 and 0.80, respectively, and the root mean squared errors (RMSEs) are 0.58 and 0.42.

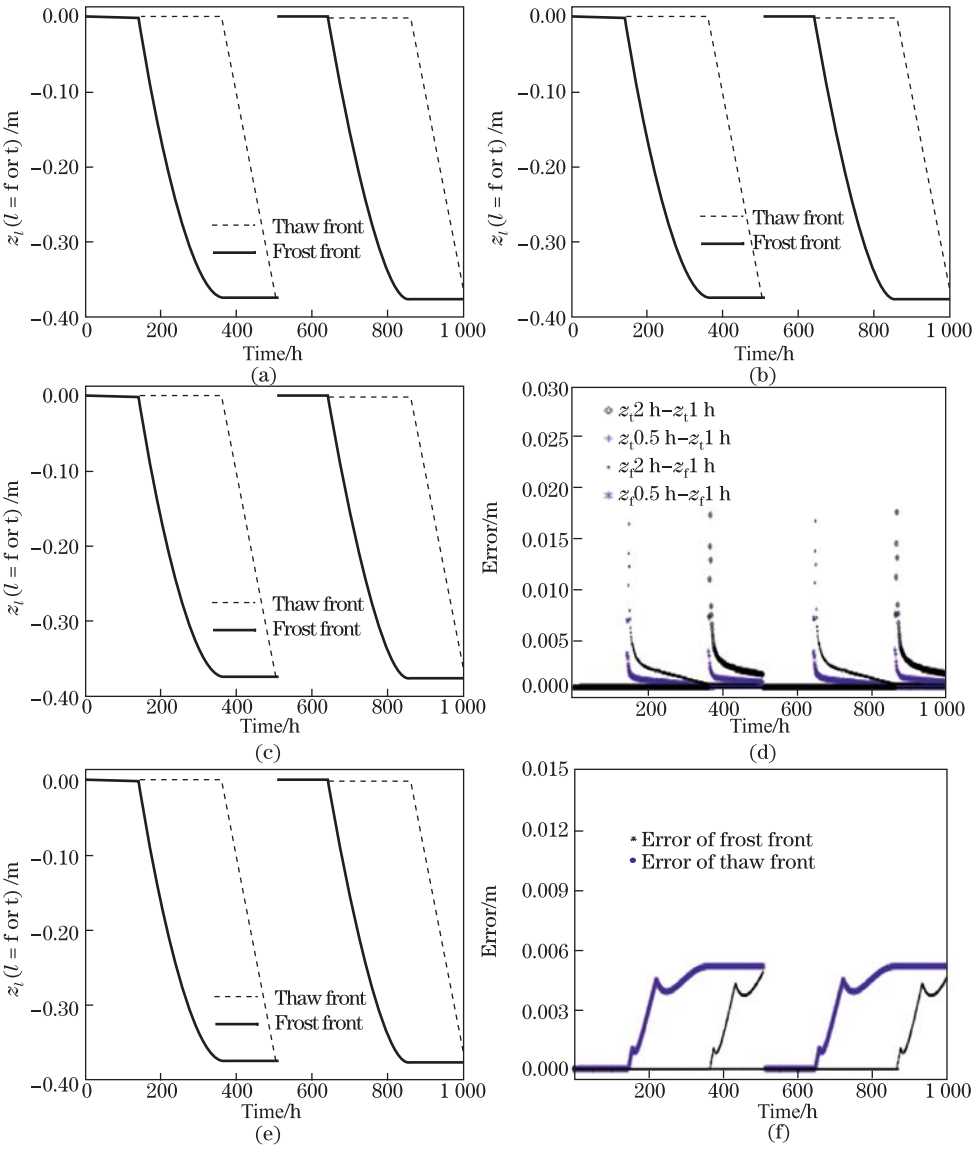

Fig. 2 Comparative tests using different time steps and different spatial resolutions: (a) time step is 0.5 h; (b) time step is 1 h; (c) time step is 2 h; (d) error with different time steps; (e) high spatial resolution (1 cm soil layer); (f) error with different spatial resolutions, where z_t2 h–z_t1 h represents error between thaw depths obtained at 2 h and 1 h, and meanings of z_t0.5 h–z_t1 h, z_f2 h–z_f1 h, and z_f0.5 h–z_f1 h are similar

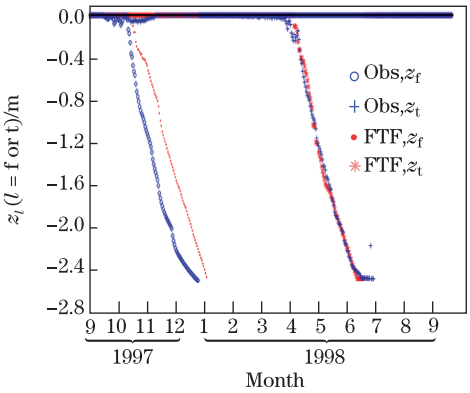

Fig. 3 FTF depths according to simulations and observations for D66 site, where "Obs" represents observations, and horizontal axis ranges from September 1, 1997 to September 22, 1998

Figure 4 shows the soil temperatures at 20 cm, 60 cm, 100 cm, and 160 cm according to the simulations of Model 1 and Model 2. Comparisons with the observations are also performed for the same time period. According to Fig. 4, the trends in the soil temperature simulated by the two models are consistent with the observations. The red lines representing Model 1 are closer to the actual values than the blue lines representing Model 2. Table 2 shows the CCs and RMSEs for the soil temperature in different soil layers using simulations of Model 1

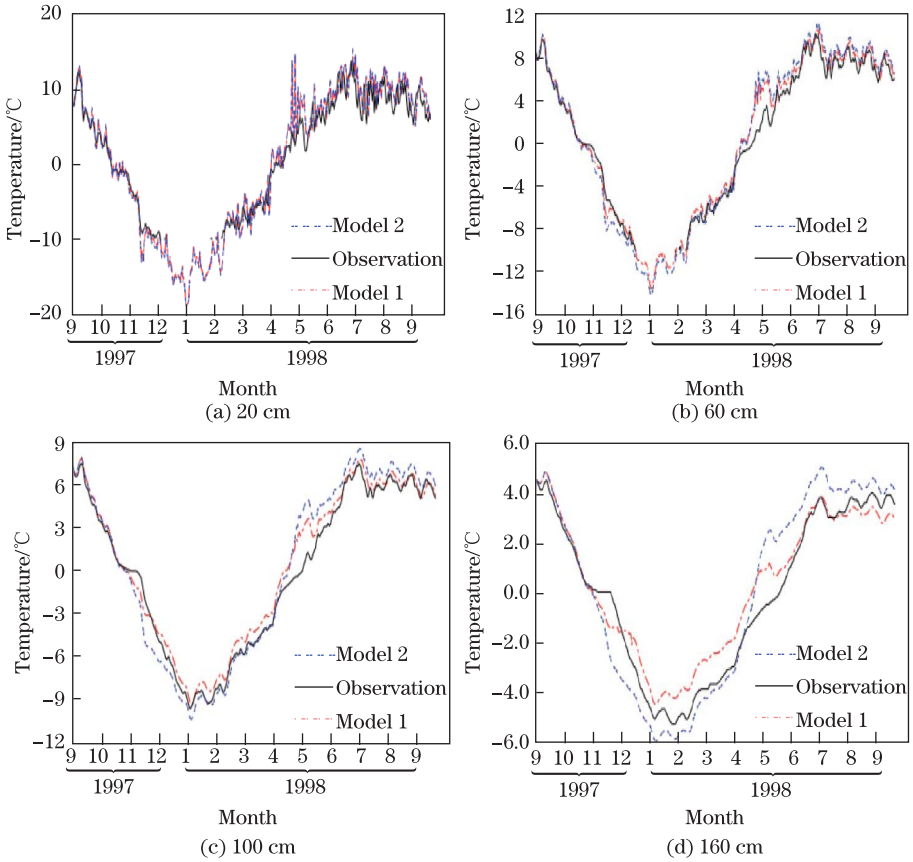

Fig. 4 Soil temperature observations and simulations obtained using Model 1 (simulation with FTFs) and Model 2 (simulation without FTFs) for D66 site: (a) 20 cm; (b) 60 cm; (c) 100 cm; (d) 160 cm, where horizontal axis ranges from September 1, 1997 to September 22, 1998

Table 2 CCs and RMSEs between simulations of Model 1 and Model 2 as well as observations in different soil layers

Soil temperature	20 cm		60 cm		100 cm		160 cm	
	CC	RMSE/°C	CC	RMSE/°C	CC	RMSE/°C	CC	RMSE/°C
Model 2	0.94	2.14	0.98	1.35	0.98	1.30	0.97	1.15
Model 1	0.94	2.05	0.98	1.04	0.99	0.85	0.97	0.79

and Model 2 and based on the observations. According to Table 2, Model 1 has lower RMSEs at depths of 20 cm, 60 cm, 100 cm, and 160 cm. Figure 4 and Table 2 demonstrate that the simulation results obtained by Model 1 are better than those using Model 2. The improvement using Model 1 compared with Model 2 is better in the lower levels than that in the upper level. This is because when the model considers the change in the FTFs, the soil temperature profile within a soil layer can be estimated according to the positions of the FTFs. Comprehensive simulations of the two models demonstrate the potential application of this algorithm to the modeling of land-surface processes.

4 Conclusions and discussion

In this study, we use a two-directional freeze and thaw algorithm to simulate the FTFs which we incorporate into the thermal diffusion equation. A local adaptive variable-grid method is used to discretize the model. We perform sensitivity tests using different time steps and spatial resolutions, which demonstrate that the proposed method is stable and that the FTFs can be tracked continuously. We perform simulations of the FTFs and soil temperature at the Qinghai-Tibet Plateau D66 site from September 1, 1997 to September 22, 1998. The simulated values fit well with the data observations collected at the D66 site. The results show that the incorporated model performs much better in the soil temperature simulation than the original thermal diffusion equation, thereby demonstrating that this algorithm can potentially be used to the modeling of land-surface processes.

Acknowledgements The data used in this study are obtained from the Sino-Japanese international cooperation project "Global Energy and Water Balance Experiment —— Qinghai-Tibet Plateau Asian Monsoon Experiment" (GAME-Tibet).

References

[1] Yi, S. H., Arain, M. A., and Woo, M. K. Modifications of a land surface scheme for improved simulation of ground freeze-thaw in northern environments. *Geophysical Research Letters*, **33**, L13501 (2006)

[2] Lin, Q., Jin, H. J., and Cheng, G. D. CH4 and CO2 emission from permafrost surface in Wudaoliang in the Tibetan Plateau (in Chinese). *Journal of Glaciology and Geocryology*, **18**, 326–327 (1996)

[3] Michaelson, G. J., Ping, C. L., and Kimble, J. M. Carbon storage and distribution in tundra soils of Arctic Alaska, U. S. A. *Arctic and Alpine Research*, **28**, 414–424 (1996)

[4] Anisimov, O. A., Shiklomanov, N. I., and Nelson, F. E. Global warming and active-layer thickness: results from tranisent general circulation models. *Global and Planetary Change*, **15**, 61–77 (1997)

[5] Pang, Q. Q., Cheng, G. D., Li, S. X., and Zhang, W. G. Active layer thickness calculation over the Qinghai-Tibet Plateau. *Cold Regions Science and Technology*, **57**, 23–28 (2009)

[6] Zhang, T. Influence of the seasonal snow cover on the ground thermal regime: an overview. *Reviews of Geophysics*, **43**, RG4002 (2005)

[7] Iwata, Y., Hirota, T., Hayashi, M., Suzuki, S., and Hasegawa, S. Effects of snow cover on soil freezing water movement, and snowmelt infiltration: a paired plot experiment. *Water Resources Research*, **46**, W09504 (2010)

[8] Harada, Y., Tsuchiya, F., Takeda, K., and Muneoka, T. Characteristics of ground freezing and thawing under snow cover based on long-term observation. *Seppyo*, **71**, 241–252 (2009)

[9] Goulden, M. L., Wofsy, S. C., Harden, J. W., Trumbore, S. E., Crill, P. M., Gower, S. T., Fries, T., Danbe, B. C., Fan, S. M., Sutton, D. J., Bazzaz, A., and Munger, J. W. Sensitivity of boreal forest carbon balance to soil thaw. *Science*, **279**, 214–217 (1998)

[10] Frauenfeld, O. W., Zhang, T. J., Barry, R. G., and Gilichinsky, D. Interdecadal changes in seasonal freeze and thaw depths in Russia. *Journal of Geophysical Rsearch*, **109**, D05101 (2004)

[11] Jumikisz, A. R. *Thermal Geotechnics*, Rutgers University Press, New Brunswick (1977)

[12] Fox, J. D. Incorporating freeze-thaw calculations into a water balance model. *Water Resources Research*, **28**, 2229–2244 (1992)

[13] Nelson, F. E., Shiklomanov, N. I., Mueller, G. R., Hinkel, K. M., Walker, D. A., and Bockheim, J. G. Estimating active layer thickness over a large region: Kuparuk River Basin, Alaska, U. S. A. *Arctic and Alpine Research*, **29**, 367–378 (1997)

[14] Li, X. and Koike, T. Frozen soil parameterization in SiB2 and its validation with GAME-Tibet observations. *Cold Regions Science and Technology*, **36**, 165–182 (2003)

[15] Woo, M. K., Arain, M. A., Mollinga, M., and Yi, S. A two-directional freeze and thaw algorithm for hydrologic and land surface modeling. *Geophysical Research Letters*, **31**, L12501 (2004)

[16] Harlan, R. L. Analysis of coupled heat-fluid transport in partially frozen soil. *Water Resources Research*, **9**, 1314–1323 (1973)

[17] Hu, H. P., Ye, B. S., Zhon, Y. H., and Tian, F. Q. A land surface model incorporated with soil freeze/thaw and its application in GAME/Tibet, China. *Science in China Series D*: *Earth Sciences*, **49**, 1311–1322 (2006)

[18] Sun, S. F. *Physics Biochemistry and Parameterization of Land Surface Model* (in Chinese), China Meteorological Press, Beijing, 53–69 (2005)

[19] Zhang, X., Sun, S. F., and Xue, Y. K. Development and testing of a frozen soil parameterization for cold region studies. *Journal of Hydrometeorology*, **8**, 690–701 (2007)

[20] Niu, G. Y. and Yang, Z. L. Effects of frozen soil on snowmelt runoff and soil water storage at a continental scale. *Journal of Hydrometeorology*, **7**, 973–952 (2006)

[21] Shang, S. H., Mai, X. M., Lei, Z. D., and Yang, S. X. *Soil Moisture Dynamics Simulation Model and Its Applications*, Science Press, Beijing, 65–85 (2009)

[22] Xie, C. W. and William, A. A simple thaw-freeze algorithm for a multi-layered soil using the Stefan equation. *Permafrost and Periglacial Processes*, **24**, 252–260 (2013)

[23] Wang, A. W., Xie, Z. H., Feng, X. B., Tian, X. J., and Qin, P. H. A soil water and heat transfer model including changes in soil frost and thaw fronts. *Science in China Series D*: *Earth Sciences*, **57**, 1325–1339 (2014)

[24] Wang, L., Koike, T., Yang, K., Jin, R., and Li, H. Frozen soil parameterization in a distributed biosphere hydrological model. *Hydrology and Earth System Sciences*, **14**, 557–571 (2010)

[25] Xie, Z. H., Song, L. Y., and Feng, X. B. A moving boundary problem derived from heat and water transfer processes in frozen and thawed soils and its numerical simulation. *Science in China Series A*: *Mathematics*, **51**, 1510–1521 (2008)

[26] Beringer, J., Lynch, A. H., Chapin, F. S., III, Mack, M., and Bonan, G. B. The representation of arctic soils in the land surface model: the importance of mosses. *Journal of Climate*, **14**, 3324–3335 (2001)

[27] Keith, W. O. and David, M. L. *Technical Description of Version* 4.5 *of the Community Land Model* (*CLM*), National Center for Atmospheric Research, Boulder (2013)

[28] Li, Q. and Sun, S. F. Development of the universal and simplified soil model coupling heat and water transport. *Science in China Series D*: *Earth Sciences*, **37**, 1522–1535 (2007)

[29] Li, Q., Sun, S. F., and Xue, Y. K. Analyses and development of a hierarchy of frozen soil models for cold region study. *Journal of Geophysical Research*: *Atmospheres*, **115**, D03107 (2010)